

Electron spin relaxation due to D'yakonov-Perel' and Elliot-Yafet mechanisms in monolayer MoS₂: Role of intravalley and intervalley processes

L. Wang and M. W. Wu*

*Hefei National Laboratory for Physical Sciences at Microscale and Department of Physics,
University of Science and Technology of China, Hefei, Anhui, 230026, China*
(Dated: September 24, 2018)

We investigate the in-plane spin relaxation of electrons due to the D'yakonov-Perel' and Elliot-Yafet mechanisms including the intra- and inter-valley processes in monolayer MoS₂. We construct the effective Hamiltonian for the conduction band using the Löwdin partition method from the anisotropic two-band Hamiltonian with the intrinsic spin-orbit coupling of the conduction band included. The spin-orbit coupling of the conduction band induces the intra- and inter-valley D'yakonov-Perel' spin relaxation. In addition, the Elliot-Yafet spin relaxation also takes place due to the interband spin mixing. We find that the D'yakonov-Perel' mechanism dominates the in-plane spin relaxation. In the framework of this mechanism, the intravalley process is shown to play a more important role at low temperature whereas the intervalley one becomes more important at high temperature. At the temperature in between, the leading process of the in-plane spin relaxation changes from the intervalley to intravalley one as the electron density increases. Moreover, we find that the intravalley process is dominated by the electron-electron Coulomb scattering even with high impurity density since the dominant term in the spin-orbit coupling is isotropic, which does not lead to the spin relaxation together with the electron-impurity scattering. This is very different from the previous studies in semiconductors and graphene.

PACS numbers: 72.25.Rb, 81.05.Hd, 71.10.-w, 71.70.Ej

I. INTRODUCTION

In the past few years, great efforts have been devoted to a new two-dimensional material, i.e., monolayer MoS₂¹⁻³ since it has a direct gap at K(K') point,⁴⁻²⁰ valley-dependent interband optical selection rule,^{11,21-25} and also good spin properties.^{9,11,14,16-20,26-28} Specifically, both the conduction and valence bands are spin splitted caused by the space inversion asymmetry.^{9,11,14,16-20,26-28} This spin splitting at K(K') point has opposite signs due to the time reversal symmetry, which makes the spintronics intriguing in this multivalley system.

Spin relaxation, which is one of the prerequisites in realizing spintronic devices, has been studied in monolayer MoS₂ very recently.^{28,29} There exist both the intravalley²⁸ and intervalley²⁹ spin relaxation processes. Specifically, Ochoa and Roldán²⁸ investigated the intravalley electron relaxation process for in-plane spins due to what they claimed **both the** D'yakonov-Perel'³⁰ (DP) and Elliot-Yafet³¹ (EY) mechanisms. However, the intravalley DP spin relaxation process contributed by the disorder is in fact absent since the isotropic low-energy two-band Hamiltonian,¹¹ i.e.,

$$H_{\mu}^i = \Delta\tau_z/2 + \lambda_v\mu\sigma_z(1 - \tau_z)/2 + t_0a_0\mathbf{k} \cdot \boldsymbol{\tau}_{\mu}, \quad (1)$$

is employed in their calculation.^{30,32} Here, $\boldsymbol{\tau}$ and $\boldsymbol{\sigma}$ are the Pauli matrices for two Bloch basis functions and spins, respectively; $\boldsymbol{\tau}_{\mu} = (\mu\tau_x, \tau_y)$; valley index $\mu = 1(-1)$ represents K(K') valley; Δ is the energy gap; λ_v is the strength of the intrinsic spin-orbit cou-

pling (SOC) of the valence band. This isotropic Hamiltonian can lead to the intravalley spin relaxation in the presence of the electron-electron Coulomb and intravalley electron-phonon scatterings. These scatterings are unfortunately absent in Ref. 28. In addition, according to the latest report by Rostami *et al.*,¹⁷ the isotropic two-band Hamiltonian becomes anisotropic when higher order terms in the momentum are taken into account. Specifically,

$$H_{\mu}^a = H_{\mu}^i + \frac{\hbar^2k^2}{4m_0}(\alpha + \beta\tau_z) + t_1a_0^2\mathbf{k} \cdot \boldsymbol{\tau}_{\mu}^*\tau_x\mathbf{k} \cdot \boldsymbol{\tau}_{\mu}^*, \quad (2)$$

in which the last term is anisotropic. This anisotropic term can cause the DP spin relaxation together with the electron-impurity scattering. Moreover, the intrinsic SOC of the conduction band [$\lambda_c\mu\sigma_z(1 + \tau_z)/2$], which provides opposite effective magnetic fields in the two valleys,^{18,33} is neglected in the above Hamiltonians [Eqs. (1) and (2)]. This SOC has been demonstrated to open an intervalley DP relaxation process for in-plane spins in the presence of intervalley electron-phonon scattering very recently by Wang and Wu.²⁹ Therefore, it is of crucial importance to give a full investigation on the spin relaxation and compare the relative importance of each mechanism in monolayer MoS₂.

In the present work, by taking into account all the relevant scatterings, we study the electron spin relaxation due to the DP and EY mechanisms with the intra- and inter-valley processes included in monolayer MoS₂ by the kinetic spin Bloch equation (KSBE) approach.³² With the anisotropic two-band Hamiltonian by Rostami

*et al.*¹⁷ [see Eq. (2)] and the intrinsic SOC of the conduction band included,^{18,33} the SOC of the conduction band near the K(K') point to the third order of the momentum is given by

$$\mathbf{\Omega}^\mu = [2\lambda_c\mu + \mu A_1 k^2 + A_2(k_x^3 - 3k_x k_y^2)]\hat{\mathbf{z}}, \quad (3)$$

which is obtained by the Löwdin partition method.^{34,35} Here, the z -axis is set to be out of the monolayer MoS₂ plane; the coefficients A_1 and A_2 are given in Appendix A. The first two terms contain valley index and therefore provide an intervalley inhomogeneous broadening³⁶ for in-plane spins, which leads to intervalley DP spin relaxation together with the intervalley scattering.^{29,37,38} In addition, the last two terms are momentum dependent, which induce not only the intervalley DP spin relaxation with the intervalley scattering but also the intravalley one with the intravalley scattering. It is noted that only the anisotropic cubic term causes the DP spin relaxation with the electron-impurity scattering.

In addition to the DP mechanism, we also include the EY one. However, the contribution of the EY mechanism to the in-plane spin relaxation is negligible compared with that of the DP one due to the marginal in-plane spin mixing. In the framework of the DP mechanism, we find that the intravalley process plays a more important role at low temperature. However, at high temperature, the intervalley process becomes more important. As for the temperature in between, we find that the leading process of the spin relaxation changes from the intervalley to intravalley one with increasing electron density. Moreover, we find that the electron-electron Coulomb scattering dominates the intravalley process even in the presence of high impurity density, due to the negligible inhomogeneous broadening from the anisotropic term in the SOC. This is very different from semiconductors³² and graphene.^{38,39}

This paper is organized as follows. In Sec. II, we introduce our model and the numerical method. Then in Sec. III, we investigate the temperature and electron-density dependences of the in-plane spin relaxation. We summarize in Sec. IV.

II. MODEL AND KSBES

In monolayer MoS₂, the effective Hamiltonian of the conduction band near the K(K') point can be written as

$$H_{\text{eff}}^\mu = \epsilon_{\mu\mathbf{k}} + \mathbf{\Omega}^\mu \cdot \boldsymbol{\sigma}/2 \quad (4)$$

where $\epsilon_{\mu\mathbf{k}} = \hbar^2\mathbf{k}^2/(2m^*)$ with m^* being the effective mass and $\mathbf{\Omega}^\mu$ is given in Eq. (3). This effective Hamiltonian is obtained by the Löwdin partition method^{34,35} up to the third order of the momentum.⁴⁰ The details are shown in Appendix A. It is noted that similar effective Hamiltonian with the cubic term neglected has been given by Kormányos *et al.*³³

We then construct the microscopic KSBES³² to study the electron spin relaxation in monolayer MoS₂. The KSBES read³²

$$\partial_t \rho_{\mu\mathbf{k}} = \partial_t \rho_{\mu\mathbf{k}}|_{\text{coh}} + \partial_t \rho_{\mu\mathbf{k}}|_{\text{scat}}, \quad (5)$$

where $\rho_{\mu\mathbf{k}}$ stand for the density matrices of electrons with the diagonal terms $\rho_{\mu\mathbf{k},\sigma\sigma} \equiv f_{\mu\mathbf{k}\sigma}$ ($\sigma = \pm\frac{1}{2}$) denoting the distribution functions and the off-diagonal ones $\rho_{\mu\mathbf{k},(\frac{1}{2})(-\frac{1}{2})} = \rho_{\mu\mathbf{k},(-\frac{1}{2})(\frac{1}{2})}^*$ being the spin coherence. The coherent terms $\partial_t \rho_{\mu\mathbf{k}}|_{\text{coh}}$ are given in Ref. 39. $\partial_t \rho_{\mu\mathbf{k}}|_{\text{scat}}$ are the scattering terms including the spin conserving terms, i.e., the electron-electron Coulomb, electron-impurity, intravalley electron-acoustic phonon, electron-optical phonon, and also the intervalley electron-phonon^{13,29} (electron-KTA, -KLA, -KTO, and -KLO) scatterings and the spin-flip terms due to the EY mechanism.³¹ Their detailed expressions can be found in Ref. 41⁴² and here we only show the electron-electron Coulomb scattering in Appendix A. The scattering matrix elements have been introduced in Ref. 29 and the spin mixing $\hat{\Lambda}_{\mu\mathbf{k},\mu'\mathbf{k}'}$ for the conduction band in the spin-flip scattering terms is given in Appendix A.

III. NUMERICAL RESULTS

In the calculation, the effective mass, calculated from Eq. (A1) in Appendix A, reads $m^* = 0.38m_0$ with m_0 being the free electron mass. The coefficients of the SOC $\lambda_c = 1.5$ meV,^{18,26,27} $A_1 = 417.94$ meV \AA^2 and $A_2 = 92.52$ meV \AA^3 , in which A_1 and A_2 are calculated according to Eqs. (A2)-(A3). The other parameters related to the two-band Hamiltonian [Eq. (2)] and scattering matrix elements are given in Ref. 17 and Ref. 29, respectively. Then we present our results by numerically solving the KSBES [Eq. (5)].³² The initial spin polarization is taken to be 2.5 % and the spin-polarization direction is set to be in the monolayer MoS₂ plane unless otherwise specified.

We first investigate the temperature dependence of the in-plane spin relaxation. The in-plane SRTs τ_s as function of temperature T with different electron densities are plotted in Fig. 1. The impurity density is taken to be $N_i = 0.1N_e$ with N_e being the electron density. We first focus on the case of $N_e = 7 \times 10^{12}$ cm⁻², i.e., Fig. 1(a). By comparing the EY (curve with +) and DP (curve with \times) SRTs, we find that the SRT due to the EY mechanism is about four orders of magnitude larger than the one due to the DP mechanism. It is noted that when we artificially increase the impurity density to $N_i = 10N_e$, the EY SRT is still two orders of magnitude larger than the DP one (not shown). This indicates that the contribution of the EY mechanism to the in-plane spin relaxation is negligible, which originates from the extremely small spin mixing as shown in Appendix A. We also find that the dominant DP SRT presents a monotonic decrease with the increase of the temperature. To understand this behavior, we calculate the SRT due to the DP

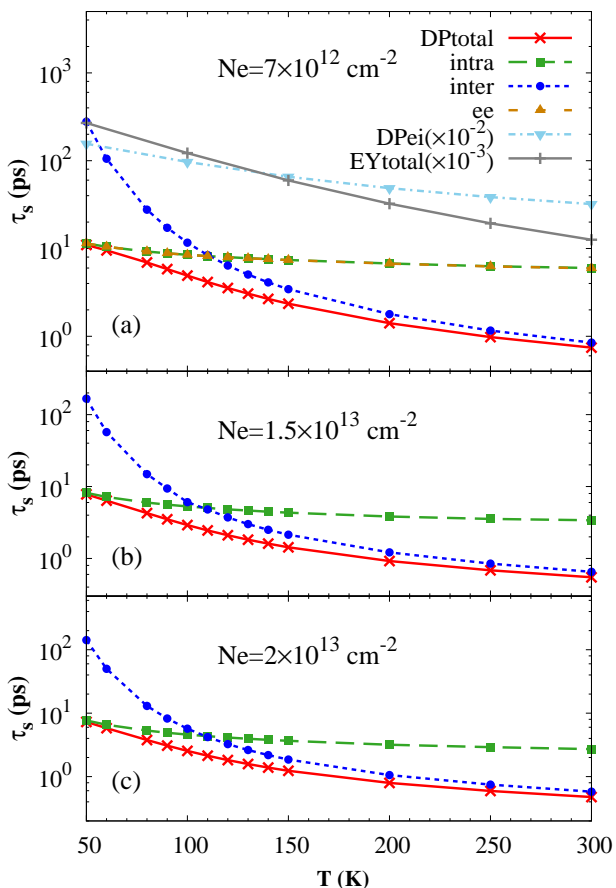


FIG. 1: (Color online) Total in-plane SRT τ_s (\times) due to the DP mechanism and that calculated with only the intravalley (\blacksquare) or intervalley process (\bullet) included as function of temperature T with (a) $N_e = 7 \times 10^{12} \text{ cm}^{-2}$; (b) $N_e = 1.5 \times 10^{13} \text{ cm}^{-2}$; and (c) $N_e = 2 \times 10^{13} \text{ cm}^{-2}$. In addition, in (a), curve with \blacktriangle (\blacktriangledown) stands for τ_s due to the DP mechanism with only the electron-electron Coulomb (electron-impurity) scattering whereas the one with $+$ represents the SRT due to the EY mechanism. The impurity density $N_i = 0.1N_e$.

mechanism with only the intravalley (\blacksquare) or intervalley (\bullet) process included, separately. It is seen that both the intra- and inter-valley²⁹ SRTs decrease with increasing temperature, leading to the decrease of the total SRT. By comparing these two processes, the intravalley one is found to be more important at low temperature whereas the intervalley one plays a more important role at high temperature.

In addition, in contrast to the rapid decrease of the SRT of the intervalley process,²⁹ we find that the intravalley SRT decreases mildly with the increase of the temperature when the electron density $N_e = 7 \times 10^{12} \text{ cm}^{-2}$ [see Fig. 1(a)]. Similar behaviors are also observed when we increase the electron density to $N_e = 1.5 \times 10^{13} \text{ cm}^{-2}$ and $N_e = 2 \times 10^{13} \text{ cm}^{-2}$ as shown in Figs. 1(b) and 1(c), respectively. To facilitate the understanding of this behavior, we calculate the intravalley

SRT with only the electron-electron Coulomb, electron-impurity, or intravalley electron-phonon scattering included, separately. We find that the intravalley process is dominated by the electron-electron Coulomb scattering [only show the case of $N_e = 7 \times 10^{12} \text{ cm}^{-2}$ in Fig. 1(a)], which is very different from the previous studies in semiconductors³² and graphene^{38,39} where the electron-impurity scattering plays a very important role in spin relaxation. Here, the marginal contribution of the electron-impurity scattering to the intravalley DP spin relaxation is due to the extremely weak inhomogeneous broadening from the anisotropic cubic term in the SOC [see Eq. (3)]. If this cubic term is further neglected, the DP spin relaxation due to the electron-impurity scattering becomes absent as previously mentioned.

The decrease of the intravalley SRT due to the electron-electron Coulomb scattering with increasing temperature in the degenerate limit⁴³ is very different from the previous studies in semiconductors,^{44–51} where a peak in the temperature dependence of the SRT from the degenerate-to-nondegenerate limit was theoretically predicted^{41,44} and experimentally realized^{45,46,50} when the spin relaxation is dominated by the electron-electron Coulomb scattering. The underlying physics can be understood from a simplified two-state model detailed in Appendix B. When the system is highly degenerate, the inhomogeneous broadening from the second term of the SOC in Eq. (3) is proportional to T^2 , which suppresses the enhancement of the electron-electron Coulomb scattering from the weakened Pauli blocking with increasing temperature.⁵² This leads to the decrease of the SRT with the increase of temperature. It is noted that when we artificially neglect the polar angle dependence of the momentum in the SOC [similar to the second term of the SOC in Eq. (3)] in semiconductors, the SRT also decreases with increasing temperature in the degenerate limit and the peak in the temperature dependence of the SRT becomes absent too (not shown).

Then we turn to study the dependence of the in-plane SRT on the electron density. As the contribution of the EY mechanism to the spin relaxation is negligible, we only calculate the total SRT and its intravalley or intervalley process due to the DP mechanism. With the impurity density $N_i = 0.1N_e$, the results at different temperatures are plotted in Fig. 2. We find that at low temperature (i.e., $T = 50 \text{ K}$), the intravalley process is always more important than the intervalley one as the electron density increases. However, at high temperature (i.e., $T = 200 \text{ K}$), the intervalley process becomes more important. As for the temperature in between (i.e., $T = 100 \text{ K}$), the leading process is found to change from the intervalley to intravalley one with the increase of electron density. In addition, we find that the total SRTs in different cases all decrease with the increase of electron density. We also find that the intervalley SRTs show a monotonic decrease with increasing electron density. This is because the intervalley electron-phonon scattering is in the weak scattering limit, which determines

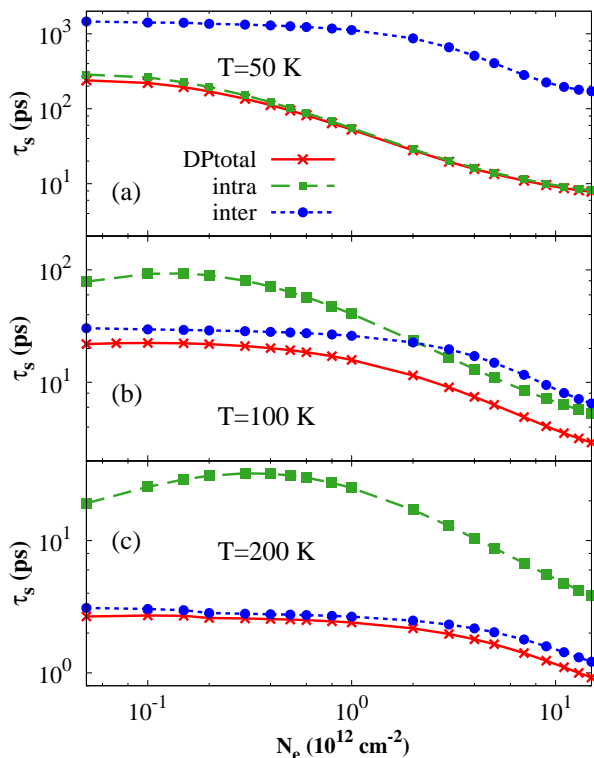


FIG. 2: (Color online) Total in-plane SRT τ_s (\times) due to the DP mechanism and that calculated with only the intravalley (\blacksquare) or intervalley process (\bullet) included as function of the electron density N_e at (a) $T = 50$ K; (b) $T = 100$ K; and (c) $T = 200$ K. The impurity density $N_i = 0.1N_e$.

the decrease of the intervalley SRT with the enhancement of the intervalley scattering as the electron density increases.²⁹ As for the intravalley process, the SRT decreases with increasing electron density at $T = 50$ K whereas a peak is observed in the density dependence of the SRT at $T = 100$ and 200 K due to the crossover from the nondegenerate-to-degenerate limit.^{41,53} The increase of the intravalley SRT at $T = 100$ and 200 K is suppressed by the decrease of the intervalley one, which leads to the decrease of the total SRT with increasing electron density.

IV. SUMMARY

In summary, we have investigated the in-plane spin relaxation of electrons in monolayer MoS₂. We construct the effective Hamiltonian for the conduction band by the Löwdin partition method including the anisotropic two-band Hamiltonian and the intrinsic SOC of the conduction band. We find that the SOC of the conduction band can lead to the intra- and inter-valley DP spin relaxation. In addition, the EY spin relaxation also exists due to the interband spin mixing.

We calculate the electron spin relaxation due to the

DP and EY mechanisms including the intra- and intervalley processes by numerically solving the KSBEs with all the relevant scatterings included. We find that the in-plane spin relaxation is dominated by the DP mechanism whereas the contribution of the EY mechanism is marginal due to the extremely weak in-plane spin mixing. For the dominant DP mechanism, the intravalley process is found to be more important at low temperature whereas the intervalley one plays a more important role at high temperature. At the temperature in between, a crossover of the leading process from the intervalley to intravalley one is shown with the increase of electron density. Moreover, we find that even in the presence of high impurity density, the intravalley process is dominated by the electron-electron Coulomb scattering since only the negligible anisotropic term in the SOC contributes to the intravalley spin relaxation due to the electron-impurity scattering. This is quite different from semiconductors and graphene. In addition, the decrease of the intravalley SRT due to the electron-electron Coulomb scattering with the increase of temperature in the degenerate limit is of great difference from the previous studies in semiconductors, where a peak in the temperature dependence of the SRT was theoretically predicted and experimentally realized when the electron-electron Coulomb scattering is dominant.

Acknowledgments

This work was supported by the National Natural Science Foundation of China under Grant No. 11334014, the National Basic Research Program of China under Grant No. 2012CB922002 and the Strategic Priority Research Program of the Chinese Academy of Sciences under Grant No. XDB01000000.

Appendix A: EFFECTIVE HAMILTONIAN AND SPIN MIXING $\hat{\Lambda}_{\mu\mathbf{k},\mu'\mathbf{k}'}$ FOR THE CONDUCTION BAND AND THE ELECTRON-ELECTRON COULOMB SCATTERING TERM

Including the anisotropic two-band Hamiltonian [Eq. (2)] and the intrinsic SOC of the conduction band, the total two-band Hamiltonian describing the low-energy conduction and valence bands near the K(K') point reads $H_{\text{tot}}^{\mu} = H_{\mu}^{\alpha} + \lambda_c \mu \sigma_z (1 + \tau_z)/2$. We define the leading part of this Hamiltonian (i.e., momentum-independent part) as $H_0 = \Delta \tau_z/2 + \lambda_v \mu \sigma_z (1 - \tau_z)/2 + \lambda_c \mu \sigma_z (1 + \tau_z)/2$. By considering the large energy gap Δ , we construct the effective Hamiltonian of the conduction band by the Löwdin partition method.^{34,35} Up to the third order of the momentum, the effective Hamiltonian is given in Eqs. (3) and (4). The effective mass m^* in Eq. (4) and the coefficients of the SOC A_1, A_2 in Eq. (3)

read

$$m^{*-1} = 2a_0^2 t_0^2 / (\hbar^2 \Delta) + (\alpha + \beta) / (2m_0), \quad (\text{A1})$$

$$A_1 = 2a_0^2 t_0^2 (\lambda_v - \lambda_c) / \Delta^2, \quad (\text{A2})$$

$$A_2 = 4t_0 t_1 a_0^3 (\lambda_v - \lambda_c) / \Delta^2. \quad (\text{A3})$$

In addition, the spin mixing $\hat{\Lambda}_{\mu\mathbf{k},\mu'\mathbf{k}'}$ for the conduction band in the spin-flip scattering due to the EY mechanism is given by $\hat{\Lambda}_{\mu\mathbf{k},\mu'\mathbf{k}'} = \hat{I} - [S_{\mu\mathbf{k}}^{(1)} S_{\mu\mathbf{k}}^{(1)\dagger} - 2S_{\mu\mathbf{k}}^{(1)} S_{\mu'\mathbf{k}'}^{(1)\dagger} + S_{\mu'\mathbf{k}'}^{(1)} S_{\mu'\mathbf{k}'}^{(1)\dagger}] / 2$ with \hat{I} standing for a 2×2 unit matrix. $S_{\mu\mathbf{k}}^{(1)}$ can be written as

$$S_{\mu\mathbf{k}}^{(1)} = -\{a_0 t_0 (\mu k_x - i k_y) + t_1 a_0^2 [(k_x^2 - k_y^2) + 2i\mu k_x k_y]\} \times [\hat{I} / \Delta + \mu \sigma_z (\lambda_v - \lambda_c) / \Delta^2]. \quad (\text{A4})$$

It is noted that the unit matrix in $\hat{\Lambda}_{\mu\mathbf{k},\mu'\mathbf{k}'}$ does not cause any spin flipping. The second term $S_{\mu\mathbf{k}}^{(1)} S_{\mu\mathbf{k}}^{(1)\dagger}$ is proportional to $[\frac{\hat{I}}{\Delta} + \frac{\mu \sigma_z (\lambda_v - \lambda_c)}{\Delta^2}]^2 = [\frac{1}{\Delta^2} + \frac{(\lambda_v - \lambda_c)^2}{\Delta^4}] \hat{I} + \frac{2(\lambda_v - \lambda_c) \mu}{\Delta^3} \sigma_z$ where only the term containing σ_z induces the spin flipping for the in-plane spins. However, this term ($\propto \Delta^{-3}$) is negligible due to the large energy gap. Similarly, the contribution of the last two terms is also marginal.

With the spin mixing $\hat{\Lambda}_{\mu\mathbf{k},\mu'\mathbf{k}'}$ included, the electron-electron Coulomb scattering term in Eq. (5) can be written as

$$\begin{aligned} \partial_t \rho_{\mu\mathbf{k}}|_{ee} = & -\pi \sum_{\mu'\mathbf{k}'\mathbf{k}''} |V_{\mathbf{k},\mathbf{k}'}^\mu|^2 \delta(\epsilon_{\mu\mathbf{k}'} - \epsilon_{\mu\mathbf{k}} + \epsilon_{\mu'\mathbf{k}''}) \\ & - \epsilon_{\mu'\mathbf{k}'' - \mathbf{k} + \mathbf{k}'} \left[\text{Tr}(\hat{\Lambda}_{\mu'\mathbf{k}'', \mu'\mathbf{k}'' - \mathbf{k} + \mathbf{k}'} \rho_{\mu'\mathbf{k}'' - \mathbf{k} + \mathbf{k}'}^<) \right. \\ & \times \hat{\Lambda}_{\mu'\mathbf{k}'' - \mathbf{k} + \mathbf{k}', \mu'\mathbf{k}''} \rho_{\mu'\mathbf{k}''}^> \hat{\Lambda}_{\mu\mathbf{k}, \mu\mathbf{k}'} \rho_{\mu\mathbf{k}'}^> \hat{\Lambda}_{\mu\mathbf{k}', \mu\mathbf{k}} \rho_{\mu\mathbf{k}}^< \\ & - \text{Tr}(\hat{\Lambda}_{\mu'\mathbf{k}'', \mu'\mathbf{k}'' - \mathbf{k} + \mathbf{k}'} \rho_{\mu'\mathbf{k}'' - \mathbf{k} + \mathbf{k}'}^> \hat{\Lambda}_{\mu'\mathbf{k}'', \mu'\mathbf{k}''} \rho_{\mu'\mathbf{k}''}^< \\ & \left. \times \rho_{\mu'\mathbf{k}''}^< \hat{\Lambda}_{\mu\mathbf{k}, \mu\mathbf{k}'} \rho_{\mu\mathbf{k}'}^< \hat{\Lambda}_{\mu\mathbf{k}', \mu\mathbf{k}} \rho_{\mu\mathbf{k}}^> \right] + \text{H.c.}, \quad (\text{A5}) \end{aligned}$$

with $|V_{\mathbf{k},\mathbf{k}'}^\mu|^2$ being the electron-electron Coulomb scattering matrix element.

Appendix B: A SIMPLIFIED TWO-STATE MODEL

We consider the intravalley in-plane spin relaxation due to the DP mechanism with only the electron-electron Coulomb scattering included. The KSBEs, i.e., Eq. (5) can be written as⁵⁴

$$\frac{\partial \rho_{\mathbf{k}}}{\partial t} + \frac{i}{2\hbar} [(2\lambda_c + A_1 k^2) \sigma_z, \rho_{\mathbf{k}}] = - \sum_{\mathbf{k}'} \frac{\rho_{\mathbf{k}} - \rho_{\mathbf{k}'}}{\tau_{|\mathbf{k}-\mathbf{k}'|}^{ee}}, \quad (\text{B1})$$

with the relaxation time approximation where $\tau_{|\mathbf{k}-\mathbf{k}'|}^{ee}$ represents the momentum scattering time due to

electron-electron Coulomb scattering. It is noted that the valley index μ is omitted since only the intravalley process is considered here. As it is difficult to solve this equation analytically, we start from a two-state model for simplicity. Specifically,

$$\frac{\partial \rho_{\mathbf{k}}}{\partial t} + \frac{i}{2\hbar} [(2\lambda_c + A_1 k^2) \sigma_z, \rho_{\mathbf{k}}] = - \frac{\rho_{\mathbf{k}} - \rho_{\mathbf{k}'}}{\tau^{ee}}, \quad (\text{B2})$$

$$\frac{\partial \rho_{\mathbf{k}'}}{\partial t} + \frac{i}{2\hbar} [(2\lambda_c + A_1 k'^2) \sigma_z, \rho_{\mathbf{k}'}] = - \frac{\rho_{\mathbf{k}'} - \rho_{\mathbf{k}}}{\tau^{ee}}, \quad (\text{B3})$$

It is noted that the isotropic approximation is employed by considering the isotropy of the SOC.⁵⁴ With $B_1 = 2\lambda_c + A_1(k^2 + k'^2)/2$, $B_2 = A_1(k^2 - k'^2)/2$ and unitary transformation $\rho_{\mathbf{k}} = e^{-iB_1 \sigma_z t / (2\hbar)} \tilde{\rho}_{\mathbf{k}} e^{iB_1 \sigma_z t / (2\hbar)}$, the above equations become

$$\frac{\partial \tilde{\rho}_{\mathbf{k}}}{\partial t} + \frac{i}{2\hbar} B_2 [\sigma_z, \tilde{\rho}_{\mathbf{k}}] = - \frac{\tilde{\rho}_{\mathbf{k}} - \tilde{\rho}_{\mathbf{k}'}}{\tau^{ee}}, \quad (\text{B4})$$

$$\frac{\partial \tilde{\rho}_{\mathbf{k}'}}{\partial t} - \frac{i}{2\hbar} B_2 [\sigma_z, \tilde{\rho}_{\mathbf{k}'}] = - \frac{\tilde{\rho}_{\mathbf{k}'} - \tilde{\rho}_{\mathbf{k}}}{\tau^{ee}}. \quad (\text{B5})$$

By defining the spin vector as $\tilde{\mathbf{S}}_{\mathbf{k}}(t) = \text{Tr}(\tilde{\rho}_{\mathbf{k}} \boldsymbol{\sigma})$, one obtains

$$\frac{\partial \tilde{\mathbf{S}}_{\mathbf{k}}}{\partial t} + \frac{B_2}{\hbar} (\tilde{\mathbf{S}}_{\mathbf{k}} \times \hat{\mathbf{z}}) = - \frac{\tilde{\mathbf{S}}_{\mathbf{k}} - \tilde{\mathbf{S}}_{\mathbf{k}'}}{\tau^{ee}}, \quad (\text{B6})$$

$$\frac{\partial \tilde{\mathbf{S}}_{\mathbf{k}'}}{\partial t} - \frac{B_2}{\hbar} (\tilde{\mathbf{S}}_{\mathbf{k}'} \times \hat{\mathbf{z}}) = - \frac{\tilde{\mathbf{S}}_{\mathbf{k}'} - \tilde{\mathbf{S}}_{\mathbf{k}}}{\tau^{ee}}. \quad (\text{B7})$$

With the initial spin polarization along x -axis $\tilde{S}_{\mathbf{k}}^x(0) = P_{k_0}$, $\tilde{S}_{\mathbf{k}'}^x(0) = P_{k'_0}$, and $\tilde{S}_{\mathbf{k}}^y(0) = \tilde{S}_{\mathbf{k}'}^y(0) = 0$, we have

$$\tilde{S}_{\mathbf{k}}^x + \tilde{S}_{\mathbf{k}'}^x = (P_{k_0} + P_{k'_0}) e^{-B_2^2 \tau^{ee} t / (2\hbar^2)}, \quad (\text{B8})$$

$$\begin{aligned} \tilde{S}_{\mathbf{k}}^y + \tilde{S}_{\mathbf{k}'}^y = & (P_{k_0} - P_{k'_0}) [e^{-B_2^2 \tau^{ee} t / (2\hbar^2)} \\ & - e^{-2t/\tau^{ee}}] B_2 \tau^{ee} / (2\hbar), \quad (\text{B9}) \end{aligned}$$

by considering $|B_2| \tau^{ee} / \hbar \ll 1$. Then, the total spin vector along the x -direction reads $S_{\mathbf{k}}^x + S_{\mathbf{k}'}^x = \text{Tr}[(\rho_{\mathbf{k}} + \rho_{\mathbf{k}'} \sigma_x)] = \cos(B_1 t / \hbar) (\tilde{S}_{\mathbf{k}}^x + \tilde{S}_{\mathbf{k}'}^x) - \sin(B_1 t / \hbar) (\tilde{S}_{\mathbf{k}}^y + \tilde{S}_{\mathbf{k}'}^y) \approx (P_{k_0} + P_{k'_0}) \cos(B_1 t / \hbar) e^{-t B_2^2 \tau^{ee} / (2\hbar^2)}$. In the degenerate limit, one obtains

$$S_{k_F}^x \approx P_{k_F 0} \cos[(2\lambda_c + A_1 k_F^2) t / \hbar] e^{-t/\tau_s(k_F)}, \quad (\text{B10})$$

with the SRT $\tau_s(k_F) = 2\hbar^6 / (A_1^2 m^{*2} k_B^2 T^2 \tau_{k_F}^{ee})$ by considering $|\epsilon_{\mathbf{k}} - \epsilon_{\mathbf{k}'}| \sim k_B T$. Here, k_F and k_B represent the Fermi wave vector and the Boltzmann constant, respectively. It is noted that the inhomogeneous broadening [i.e., $A_1^2 m^{*2} k_B^2 T^2 / (2\hbar^6)$] is proportional to T^2 . In addition, $1/\tau_{k_F}^{ee} \propto \ln(E_F/k_B T) T^2 / E_F$ in the degenerate limit with E_F being the Fermi energy.⁵² Therefore, one has $\tau_s(k_F) \propto \ln(E_F/k_B T) / E_F$.

- * Author to whom correspondence should be addressed; Electronic address: mwwu@ustc.edu.cn.
- ¹ K. S. Novoselov, D. Jiang, F. Schedin, T. J. Booth, V. V. Khotkevich, S. V. Morozov, and A. K. Geim, *PNAS* **102**, 10451 (2005).
 - ² H. S. S. R. Matte, A. Gomathi, A. K. Manna, D. J. Late, R. Datta, S. K. Pati, and C. N. R. Rao, *Angew. Chem.* **122**, 4153 (2010).
 - ³ B. Radisavljevic, A. Radenovic, J. Brivio, V. Giacometti, and A. Kis, *Nature Nanotech.* **6**, 147 (2011).
 - ⁴ A. Splendiani, L. Sun, Y. Zhang, T. Li, J. Kim, C.-Y. Chim, G. Galli, and F. Wang, *Nano Lett.* **10**, 1271 (2010).
 - ⁵ K. F. Mak, C. Lee, J. Hone, J. Shan, and T. F. Heinz, *Phys. Rev. Lett.* **105**, 136805 (2010).
 - ⁶ G. Eda, H. Yamaguchi, D. Voiry, T. Fujita, M. Chen, and M. Chhowalla, *Nano Lett.* **11**, 5111 (2011).
 - ⁷ T. Korn, S. Heydrich, M. Hirmer, J. Schmutzler, and C. Schüller, *Appl. Phys. Lett.* **99**, 102109 (2011).
 - ⁸ J. K. Ellis, M. J. Lucero, and G. E. Scuseria, *Appl. Phys. Lett.* **99**, 261908 (2011).
 - ⁹ Z. Y. Zhu, Y. C. Cheng, and U. Schwingenschlögl, *Phys. Rev. B* **84**, 153402 (2011).
 - ¹⁰ Q. H. Wang, K. K. Zadeh, A. Kis, J. N. Coleman, and M. S. Strano, *Nature Nanotech.* **7**, 699 (2012).
 - ¹¹ D. Xiao, G.-B. Liu, W. Feng, X. Xu, and W. Yao, *Phys. Rev. Lett.* **108**, 196802 (2012).
 - ¹² W. S. Yun, S. W. Han, S. C. Hong, I. G. Kim, and J. D. Lee, *Phys. Rev. B* **85**, 033305 (2012).
 - ¹³ K. Kaasbjerg, K. S. Thygesen, and K. W. Jacobsen, *Phys. Rev. B* **85**, 115317 (2012).
 - ¹⁴ T. Cheiwchanhannangij and W. R. L. Lambrecht, *Phys. Rev. B* **85**, 205302 (2012).
 - ¹⁵ X. Li, J. T. Mullen, Z. Jin, K. M. Borysenko, M. B. Nardelli, and K. W. Kim, *Phys. Rev. B* **87**, 115418 (2013).
 - ¹⁶ H. Shi, H. Pan, Y.-W. Zhang, and B. I. Yakobson, *Phys. Rev. B* **87**, 155304 (2013).
 - ¹⁷ H. Rostami, A. G. Moghaddam, and R. Asgari, *Phys. Rev. B* **88**, 085440 (2013).
 - ¹⁸ A. Kormányos, V. Zólyomi, N. D. Drummond, P. Rakyta, G. Burkard, and V. I. Fal'ko, *Phys. Rev. B* **88**, 045416 (2013).
 - ¹⁹ E. Cappelluti, R. Roldán, J. A. S.-Guillén, P. Ordejón, and F. Guinea, *Phys. Rev. B* **88**, 075409 (2013).
 - ²⁰ F. Zahid, L. Liu, Y. Zhu, J. Wang, and H. Guo, *AIP Advances* **3**, 052111 (2013).
 - ²¹ T. Cao, G. Wang, W. Han, H. Ye, C. Zhu, J. Shi, Q. Niu, P. Tan, E. Wang, B. Liu, and J. Feng, *Nature Commun.* **3**, 887 (2012).
 - ²² H. Zeng, J. Dai, W. Yao, D. Xiao, and X. Cui, *Nature Nanotech.* **7**, 490 (2012).
 - ²³ K. F. Mak, K. He, J. Shan, and T. F. Heinz, *Nature Nanotech.* **7**, 494 (2012).
 - ²⁴ G. Sallen, L. Bouet, X. Marie, G. Wang, C. R. Zhu, W. P. Han, Y. Lu, P. H. Tan, T. Amand, B. L. Liu, and B. Urbaszek, *Phys. Rev. B* **86**, 081301(R) (2012).
 - ²⁵ D. Lagarde, L. Bouet, X. Marie, C. R. Zhu, B. L. Liu, T. Amand, and B. Urbaszek, arXiv:1308.0696.
 - ²⁶ E. S. Kadantsev and P. Hawrylak, *Solid State Commun.* **152**, 909 (2012).
 - ²⁷ K. Kośmider and J. F. Rossier, *Phys. Rev. B* **87**, 075451 (2013).
 - ²⁸ H. Ochoa and R. Roldán, *Phys. Rev. B* **87**, 245421 (2013).
 - ²⁹ L. Wang and M. W. Wu, arXiv:1305.3361.
 - ³⁰ M. I. D'yakonov and V. I. Perel', *Zh. Eksp. Teor. Fiz.* **60**, 1954 (1971) [*Sov. Phys. JETP* **33**, 1053 (1971)]; *Fiz. Tverd. Tela (Leningrad)* **13**, 3581 (1971) [*Sov. Phys. Solid State* **13**, 3023 (1972)].
 - ³¹ Y. Yafet, *Phys. Rev.* **85**, 478 (1952); R. J. Elliot, *ibid.* **96**, 266 (1954).
 - ³² M. W. Wu, J. H. Jiang, and M. Q. Weng, *Phys. Rep.* **493**, 61 (2010).
 - ³³ A. Kormányos, V. Zólyomi, N. D. Drummond, and G. Burkard, arXiv:1310.7720.
 - ³⁴ P. O. Löwdin, *J. Chem. Phys.* **19**, 1396 (1951).
 - ³⁵ R. Winkler, *Spin-Orbit Coupling Effects in Two-Dimensional Electron and Hole Systems* (Springer, Berlin, 2003).
 - ³⁶ M. W. Wu and C. Z. Ning, *Eur. Phys. J. B* **18**, 373 (2000); M. W. Wu, *J. Phys. Soc. Jpn.* **70**, 2195 (2001).
 - ³⁷ P. Zhang, Y. Zhou, and M. W. Wu, *J. Appl. Phys.* **112**, 073709 (2012).
 - ³⁸ L. Wang and M. W. Wu, *Phys. Rev. B* **87**, 205416 (2013).
 - ³⁹ Y. Zhou and M. W. Wu, *Phys. Rev. B* **82**, 085304 (2010).
 - ⁴⁰ It is noted that the trigonal warping term (i.e., spinless cubic term) is neglected since its contribution to the energy of the conduction band is marginal.
 - ⁴¹ J. H. Jiang and M. W. Wu, *Phys. Rev. B* **79**, 125206 (2009).
 - ⁴² Note that the scatterings in Ref. 41 are in bulk system and one has to transform them to two-dimensional case. In addition, one also has to transform these scatterings from single valley to two valleys, which can refer to Ref. 39.
 - ⁴³ The Fermi temperature $T_F \sim 256$ K, 548 K and 731 K corresponding to $N_e = 7 \times 10^{12} \text{ cm}^{-2}$, $1.5 \times 10^{13} \text{ cm}^{-2}$ and $2 \times 10^{13} \text{ cm}^{-2}$, respectively.
 - ⁴⁴ J. Zhou, J. L. Cheng, and M. W. Wu, *Phys. Rev. B* **75**, 045305 (2007).
 - ⁴⁵ W. J. H. Leyland, G. H. John, R. T. Harley, M. M. Glazov, E. L. Ivchenko, D. A. Ritchie, I. Farrer, A. J. Shields, and M. Henini, *Phys. Rev. B* **75**, 165309 (2007).
 - ⁴⁶ X. Z. Ruan, H. H. Luo, Y. Ji, Z. Y. Xu, and V. Umansky, *Phys. Rev. B* **77**, 193307 (2008).
 - ⁴⁷ P. Zhang and M. W. Wu, *Phys. Rev. B* **80**, 155311 (2009).
 - ⁴⁸ Y. Zhou, J. H. Jiang, and M. W. Wu, *New J. Phys.* **11**, 113039 (2009).
 - ⁴⁹ B. Y. Sun, P. Zhang, and M. W. Wu, *J. Appl. Phys.* **108**, 093709 (2010).
 - ⁵⁰ L. F. Han, Y. G. Zhu, X. H. Zhang, P. H. Tan, H. Q. Ni, and Z. C. Niu, *Nanoscale Res. Lett.* **6**, 84 (2011).
 - ⁵¹ L. Wang and M. W. Wu, *Phys. Rev. B* **85**, 235308 (2012).
 - ⁵² M. M. Glazov and E. L. Ivchenko, *Zh. Eksp. Teor. Fiz.* **126**, 1465 (2004) [*JETP* **99**, 1279 (2004)].
 - ⁵³ M. Krauß, H. C. Schneider, R. Bratschitsch, Z. Chen, and S. T. Cundiff, *Phys. Rev. B* **81**, 035213 (2010).
 - ⁵⁴ It is noted that we neglect the cubic term of the SOC since its contribution to the intravalley spin relaxation is marginal when only the electron-electron Coulomb scattering is included.